Hindawi
Mathematical Problems in Engineering
Volume 2018, Article ID 9412350, 12 pages
https://doi.org/10.1155/2018/9412350

Research Article

Research on Initial Installed Power Loss of a Certain Type of Turbo-Shaft Engine Using Data Mining and Statistical Approach

Heng Wu,[1] **Benwei Li**,[1] **Shufan Zhao**,[1] **Xinyi Yang**,[1] **and Hanqiang Song**[2]

[1]*Aviation Foundation College, Naval Aviation University, Yantai 264001, China*
[2]*Institute of Aviation Equipment, Naval Academy of Armament, Shanghai 200436, China*

Correspondence should be addressed to Heng Wu; wuheng89810@163.com

Received 28 June 2018; Accepted 4 September 2018; Published 24 September 2018

Academic Editor: Francesco Riganti-Fulginei

The installed positions of three domestic turbo-shaft engines mounted on a certain type of ship-borne helicopter interfere with the intake air flow of the engines, resulting in a decline of engine performance after initial installation. Due to the difference of load and adjustment method under the bench and installed conditions, it is necessary to study the change in gas turbine power rather than output shaft power of the engine before and after installation to evaluate the engine initial installed power loss. In this paper, quantum-behaved particle swarm optimization (QPSO) is applied to optimize the calculation of gas turbine power at different steady states based on the component-level aerodynamic thermal model of gas generator. Then, extreme learning machine (ELM) is adopted for regressive identification of the established gas generator state assessment model based on data mining and the identification model is applied to engine installed condition. Finally, statistical analysis of engine initial installed gas turbine power loss at three installed positions is carried out, respectively. Results show that the values of engine initial installed gas turbine power loss at three installed positions all conform to the normal distribution, the mean values are 1.658%, 9.828%, and 5.089%, respectively, and a confidence interval with 95% confidence level of the mean values are (1.388%, 1.928%), (9.178%, 10.478%) and (4.308%, 5.870%), which can provide references for determining the power monitoring thresholds after engine installation.

1. Introduction

The actual available power of turbo-shaft engine after installation is not only one of the main factors that determine the maximum flying speed, maximum climb rate and the use ceiling of helicopter, but also an important reference standard for setting health monitoring threshold of the engine [1, 2]. A certain type of ship-borne helicopter assembles with three domestic turbo-shaft engines. Due to the impact of installed positions and use environment, the actual available power of each engine after initial installation is lower than the power in engine bench test condition [3], and this power loss is analyzed. Usually, engine output shaft power is used to evaluate the engine performance. However, for a certain type of turbo-shaft engine, the output shaft is connected to a hydraulic dynamometer on engine bench test condition, and the hydraulic dynamometer does not have a feedback regulation. While, under installed condition, the engine output shaft is connected to the reducer and rotor, the rotor speed regulator adjusts the state of engine to keep the rotor speed constant. The differences in load and adjustment method make it impossible to determine the change value of engine output shaft power in the same state before and after installation to analyze the initial installed power loss caused by the disturbance of intake air flow. So it is necessary to evaluate the decline of doing work capacity of the engine after initial installation according to the change of gas turbine power [4, 5].

Gas turbine power of the engine is usually not measurable. At present, calculations of gas turbine power for different types of engines at home and abroad basically adopt the methods of aerodynamic thermal modeling [6–13] and simulation modeling [14, 15], among which the typical ones are the following: Coban et al. [6] combined the aerodynamic performance calculation method with bench test data to evaluate the energy and dynamic characteristics of a military turbo-shaft engine. Zhu [7] applied a differential evolution algorithm to optimize the computational performance of

the aerodynamic thermal model with the consideration of machining error and component performance degradation. Onder et al. [8] adopted numerical methods to analyze power generation and installed application of turbo-shaft engines from the perspective of energy and dynamics. Nkoi et al. [14] established simulation model for performance calculation of an original engine and the corresponding modified engine. Ghoreyshi et al. [15] proposed a method of computational fluid dynamics (CFD) flow field simulation for engine gas path components to calculate the engine output shaft power. All of the above studies require adequate engine design and measurable parameter data, but, under installed condition, few measurable parameters of a certain type of turbo-shaft engine limit the application of methods of aerodynamic thermal modeling and simulation modeling.

In recent years, there have been a growing number of data-driven model identification studies [16–19]. Lu et al. [16] proposed a novel wiener model constructed by an optimized kernel extreme learning machine to identify the dynamic and static behavior of a gas turbine engine. Pan et al. [17] applied an artificial neural network for identifying the engine's nonlinear auto regressive model with exogenous inputs. However, none of the above studies have taken gas turbine power as a parameter of identification model, coupled with the particularities of mission requirements; there is almost no research on initial installed gas turbine power loss of a certain type of turbo-shaft engine according to the literatures that have been reported.

To address this problem, in this study, quantum-behaved particle swarm optimization (QPSO) was applied to optimize the calculation of gas turbine power at different steady states based on aerodynamic thermal model of gas generator, then the converted gas generator rotor speed was set as an input parameter, and the converted gas turbine outlet temperature and the converted gas turbine power were set as output parameters, to establish a gas generator state assessment model. In combination with the selected sample data, extreme learning machine (ELM) was adopted for regressive identification of the model, and then the identification model is applied to engine installed condition. Finally, statistical analysis of engine initial installed gas turbine power loss at three installed positions had been carried out, respectively.

The rest of the paper is organized as follows. Section 2 gives an introduction of calculation method of gas turbine power based on QPSO. Methodology for the study of initial installed gas turbine power loss is overviewed in Section 3 and then a specific research process is proposed. Section 4 presents the calculation and statistical analysis results. The conclusion is followed in Section 5.

2. Optimized Gas Turbine Power Calculation Method

2.1. Brief of QPSO. Particle Swarm Optimization (PSO) [20] was first proposed by Eberhart and Kennedy in the United States in 1995. It is a population-based evolutionary algorithm that simulates the bird flocking process and believes that information sharing among individuals in a population can provide evolutionary advantages, and cooperation as well as competition among individuals can solve the optimization problem. Based on PSO, QPSO [21] was proposed through the introduction of quantum mechanics principle. In quantum space, the state of particles is described by wave function, the Schrödinger equation is solved to obtain the probability density function of particles appearing at a certain point, and the particle search position is determined by the probability density function. The algorithm discards the particle velocity, so it is not only simple, but also has good stability as well as strong global search and optimization capabilities. The search equation for particle's movement can be expressed as

$$x_{ij}^{k+1} = P_{ij}^{k} \pm \beta^{k} \left| {m_{\text{best}}}_{j}^{k} - x_{ij}^{k} \right| \ln\left(\frac{1}{u_{ij}^{k}}\right) \tag{1}$$

$$P_{ij}^{k} = \varphi_{ij}^{k} {p_{\text{best}}}_{ij}^{k} + \left(1 - \varphi_{ij}^{k}\right) {g_{\text{best}}}_{j}^{k} \tag{2}$$

$${m_{\text{best}}}_{j}^{k} = \frac{1}{N} \sum_{i=1}^{N} {p_{\text{best}}}_{ij}^{k} \tag{3}$$

$$\beta^{k} = \frac{(1 - 0.5)(T - k)}{T} + 0.5 \tag{4}$$

where $i = 1, 2, \cdots, N$, $j = 1, 2, \cdots, D$, $k = 1, 2, \cdots, T$, N is the population of particles, D is the particles' dimension in solution space, T is the total number of iterations. $\boldsymbol{p}_{\textbf{best}\boldsymbol{i}}$ represents the best position of the ith particle and $\boldsymbol{g}_{\textbf{best}}$ is the best position of the population. $\boldsymbol{m}_{\textbf{best}}$ denotes the mean best position defined as the mean of all the best positions of the population. P_{ij} is the local attractor of ith particle to jth dimension. φ and u are the random number distributed uniformly in $(0, 1)$, respectively. x_{ij} is jth dimension in ith particle's position. The plus and minus sign in (1) is determined according to the comparison between a random number in $(0, 1)$ and 0.5 before the position of each particle is updated. If the random number in $(0, 1)$ is less than 0.5, the plus sign is taken; otherwise the minus sign is taken. β is called contraction-expansion coefficient, which is the only control parameter of QPSO and adopts the linear decreasing strategy shown by (4).

Relevant studies have proved that QPSO shows better convergence performance than some other algorithms such as PSO and genetic algorithm in solving some typical optimization problems [21].

2.2. Calculation Method of Gas Turbine Power Based on QPSO. In this study, we focus on a two-shaft turbo-shaft engine with a free turbine (for confidentiality reasons the engine type is omitted). A schematic diagram of studied turbo-shaft engine is displayed in Figure 1, in which the gas generator shown in the dashed box is mainly composed of an intake port, a combined compressor, a combustion chamber, a gas turbine, and the front-end attachment transmissions including starter generator transmission, fuel regulator, and oil pump transmission. The power emitted by gas turbine drives the operation of compressor and front-end attachment transmissions. The numbers in the figure stand for the inlet or outlet of different components. For example, "3" stands for the outlet of combined compressor or the inlet

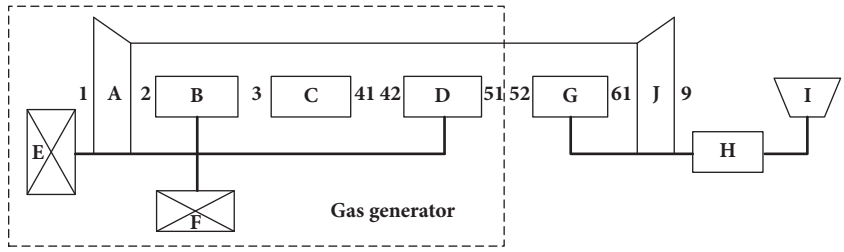

Figure 1: Schematic of studied turbo-shaft engine. (A) Intake port; (B) combined compressor; (C) combustion chamber; (D) gas turbine; (E) starter generator transmission; (F) fuel regulator and oil pump transmission; (G) free turbine; (H) reducer; (I) rotor or dynamometer; (J) tail nozzle.

of combustion chamber and "51" stands for the outlet of gas turbine.

When engine is operating under steady states, the common working conditions on aerodynamics and rotor dynamics must be followed between components. Combining the component-level aerodynamic thermal model [7] of gas generator with the collected engine bench test parameter data, including atmospheric temperature t_0, atmospheric pressure p_0, fuel consumption of combustion chamber W_f, intake air flow W_0, total pressure of compressor outlet p_3, and gas generator rotor speed n_g, the parameter values of each component's inlet and outlet section can be achieved through calculation, especially gas turbine outlet temperature T_5 and gas turbine power P_{gt}.

Considering that this type of engine was modified from the prototype, only compressor component characteristics were tested, while gas turbine was adjusted only according to the performance change of the engine under bench test condition, and gas turbine component characteristics were not tested individually after the adjustment, coupled with the error in engine manufacturing and assembly process, the component-level aerodynamic thermal model of gas generator needs to be modified to obtain an optimized, more accurate value of P_{gt}. Since sensitivity of the target performance parameters to the selected component characteristic parameters to be modified has the most direct influence on the model correction accuracy, and the compressor working state and performance can be determined with high accuracy based on measured data and the component characteristics obtained from compressor characteristic test, change of gas turbine component characteristics directly determines the performance change of gas generator. Therefore, the critical parameters that affect the calculation accuracy of gas generator performance are gas turbine pressure-drop ratio π_{gt} and gas turbine efficiency η_{gt}. In this study, the model simplification and the inaccuracy of component characteristics all boil down to the modification of gas turbine component characteristic parameters, and take π_{gt} and η_{gt} as parameters to be optimized individually. Power balance of gas generator and error between the calculated and measured values of gas turbine outlet temperature make up the target equation which means that

$$F = \alpha\left(P_{gt} - \left(P_c + P_f\right)\right) + \beta\left(T_5 - T_{5s}\right) \tag{5}$$

where P_c indicates the power absorbed by the compressor and P_f represents sum of the power consumed by front-end attachment transmissions, its value in engine design point is 18 kW and minor adjustments to it are performed to get the values of P_f in other steady states according to n_g and characteristics of parts in front-end attachments. T_5 and T_{5s} are calculated and measured values of gas turbine outlet temperature, respectively. In order to simplify the calculation, the weighting coefficients α and β are all set to 1.

The combination of π_{gt} and η_{gt} which makes the objective function value minimum is the solution obtained by optimization algorithm.

In this paper, QPSO was invited to optimize the calculation of gas turbine power at different steady states. QPSO first generates a population of particles, and the number of particles usually takes 30-50. Each particle $\boldsymbol{X_i} = [\pi_{gt,i}, \eta_{gt,i}]$ in the population denotes a potential solution consisting of the component characteristic parameters to be optimized. All elements of a particle are initialized randomly into continuous values between 0 and 1. Since each element in the particle has different meaning and different range, it is necessary to convert them into their real values before being input to the aerodynamic thermal model for calculation.

For π_{gt}, it is given by

$$z_{i1} = \left(z_\pi^{\max} - z_\pi^{\min}\right) X_{i1} + z_\pi^{\min} \tag{6}$$

where $z_\pi^{\max} = 4$ and $z_\pi^{\min} = 1$ are the upper and lower boundary values of gas turbine pressure-drop ratio π_{gt}, respectively.

For η_{gt}, it is given by

$$z_{i2} = \left(z_\eta^{\max} - z_\eta^{\min}\right) X_{i2} + z_\eta^{\min} \tag{7}$$

where $z_\eta^{\max} = 0.89$ and $z_\eta^{\min} = 0.82$ are the upper and lower boundary values of gas turbine efficiency η_{gt}, respectively.

Then, input the converted π_{gt} and η_{gt} as well as the measured steady state data of n_g, W_f, t_0, p_0, W_0, and p_3 in engine bench test to the component-level aerodynamic thermal model of gas generator, and T_5, P_{gt}, and P_c can be achieved through calculation. In combination with the data P_f and T_{5s} measured at the same steady state, QPSO evaluates the advantages and disadvantages of given parameters to be optimized according to the fitness function value which is calculated by the objective function shown in (5), and the goal

of QPSO is to minimize the fitness function value. When the iterative optimization of the algorithm meets the set precision requirement, that is $F(\boldsymbol{X}_i) < \sigma = 0.001$, or reaches the set maximum number of iterations, stop the iteration and output the optimal solution $\boldsymbol{g}_{\mathbf{best}}$. Otherwise, update each particle's best previous position $\boldsymbol{p}_{\mathbf{best}i}$ and the population's global best position $\boldsymbol{g}_{\mathbf{best}}$, calculate the local attractor P_i and mean best position $\boldsymbol{m}_{\mathbf{best}}$ of each particle using (2) and (3), and then update particle' new position according to (1), finally repeat the process of calculation on fitness function value and iterative optimization. After the optimized calculation, P_{gt} of a steady state can be obtained.

3. Methodology for the Study of Initial Installed Gas Turbine Power Loss

3.1. Brief of ELM. ELM is an excellent feed-forward neural network algorithm with single hidden layer. It only needs to set the input weight and the number of hidden layer nodes to generate a unique optimal solution so that its learning efficiency increases dramatically. Only one ELM can realize multi-input multi-output model identification, the complexity of the algorithm is low; meanwhile the identification accuracy of the model is high [22, 23].

For N arbitrary distinct samples $(\boldsymbol{x_i}, \boldsymbol{y_i})$, where $\boldsymbol{x_i} = [x_{i1}, x_{i2}, \ldots, x_{in}]^{\mathrm{T}} \in \mathbf{R}^n$ is a $n \times 1$ dimensional vector and $\boldsymbol{y_i} = [y_{i1}, y_{i2}, \ldots, y_{im}]^{\mathrm{T}} \in \mathbf{R}^m$ is a $m \times 1$ dimensional target vector, standard SLFN with $\widetilde{N}$ hidden neurons and activation function $g(x)$ can approximate these N samples with high accuracy which means that

$$\sum_{i=1}^{\widetilde{N}} \boldsymbol{\alpha_i} g_i \left(\boldsymbol{w_i} \cdot \boldsymbol{x_j} + \boldsymbol{b_i}\right) = \boldsymbol{y_j}, \quad j = 1, 2, \ldots, N \tag{8}$$

Equation (8) can be simplified as $\boldsymbol{H\alpha} = \boldsymbol{Y}$, where $\boldsymbol{H}$ is the hidden layer output matrix and $\boldsymbol{\alpha}$ is the weight vector connecting the hidden layer nodes and the output nodes. $\boldsymbol{w}$ is the weight vector connecting the input nodes and the hidden layer nodes. $\boldsymbol{b}$ denotes the bias of hidden layer nodes. $\boldsymbol{Y}$ is the matrix of desired output. The determination of the output weights is to find the least square solution with minimum norm to the linear system $\boldsymbol{H\alpha} = \boldsymbol{Y}$, which can be expressed as

$$\widetilde{\boldsymbol{\alpha}} = \boldsymbol{H}^{+}\boldsymbol{Y} = \left(\boldsymbol{H}^{\mathrm{T}}\boldsymbol{H}\right)^{-1}\boldsymbol{H}^{\mathrm{T}}\boldsymbol{Y} \tag{9}$$

where $\boldsymbol{H}^{+}$ is the Moore-Penrose generalized inverse of matrix $\boldsymbol{H}$.

3.2. Identification of Gas Generator State Assessment Model. Gas turbine power and gas turbine outlet temperature are the principal parameters for evaluating engine gas generator performance. The former parameter characterizes the doing work capacity of engine gas generator, and the latter one determines the usage time of engine's different states as well as the life of components. Therefore, gas turbine power and gas turbine outlet temperature are set as output parameters of the gas generator state assessment model. When the engine gradually rises from the ground idle state to the maximum state, parameters related to state change of the engine all increase accordingly. Therefore, only gas generator rotor speed is selected as input parameter of the gas generator state assessment model to characterize the different steady states of the engine. In addition, during the actual operation, state parameters and performance parameters of the engine are affected by different engine operating environment. In order to facilitate installed application of the model in the later period, the input and output parameters of the model are all converted to standard atmospheric condition (P_0 = 101325Pa, T_0 = 288.15K), as is listed in Table 1.

Table 1: Input and output parameters of the model.

Parameters	Unit	type
$n_{g,c}$	r/min	Input
$P_{gt,c}$	kW	Output
$T_{5s,c}$	°C	Output

10 turbo-shaft engines of the same type are selected, and optimized calculations are carried out for 5 typical steady states of each engine based on engine bench acceptance test data, respectively. The theoretical converted gas generator rotor speed of the 5 typical steady states are 25000 r/min, 30000 r/min, 31500 r/min, 32400 r/min and 33400 r/min, data selections of different steady states are according to the constant throttle position or fuel consumption basically, as well as the stability of gas generator rotor speed. All the selected data are within a certain range of the corresponding theoretical converted speed of each typical steady state. After the optimized calculations, convert n_g, P_{gt} and T_{5s} of each steady state to standard atmospheric condition. Then, a total of 50 sample data points make up the training and validation sample sets of the gas generator state assessment model, and ELM is invited to perform regressive identification of the model.

ELM can realize the multi-input multi-output model identification, in this application, $\boldsymbol{y} \in \mathbf{R}^m$ denotes the target vector composed by model output parameters $P_{gt,c}(k)$ and $T_{5s,c}(k)$, $\boldsymbol{x} \in \mathbf{R}^n$ indicates the vector composed by model input parameter $n_{g,c}(k)$, the core idea of ELM for identifying the gas generator state assessment model is as follows: for unknown nonlinear function $\boldsymbol{y} = f(\boldsymbol{x})$, along with N arbitrary distinct samples $(\boldsymbol{x_i}, \boldsymbol{y_i})$, seek a function $\widetilde{f}$ that minimizes the root mean square error between the network output vector $\widetilde{\boldsymbol{y}} = \widetilde{f}(\boldsymbol{x})$ of ELM and the target vector $\boldsymbol{y}$.

Network structure of ELM is displayed in Figure 2, when ELM performs function approximation, the established SLFNs with $\widetilde{N}$ hidden neurons and sigmoid activation function $g(x)$ can approximate the N samples with high accuracy which means that

$$\sum_{i=1}^{\widetilde{N}} \boldsymbol{\alpha_i} g_i \left(\boldsymbol{w_i} \cdot \boldsymbol{x_j} + \boldsymbol{b_i}\right) = \boldsymbol{y_j}, \quad j = 1, 2, \ldots, N \tag{10}$$

Its matrix representation is

$$\boldsymbol{H\alpha} = \boldsymbol{y} \tag{11}$$

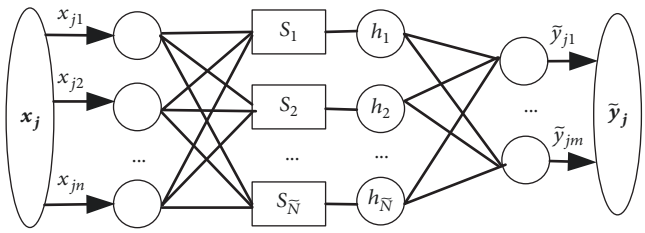

Figure 2: Network structure of ELM.

$$\begin{aligned}
&\boldsymbol{H}\left(\boldsymbol{w}_1,\cdots,\boldsymbol{w}_{\widetilde{N}},b_1,\cdots,b_{\widetilde{N}},\boldsymbol{x}_1,\cdots,\boldsymbol{x}_N\right)\\
&=\begin{bmatrix} g\left(\boldsymbol{w}_1\cdot\boldsymbol{x}_1+b_1\right) & \cdots & g\left(\boldsymbol{w}_{\widetilde{N}}\cdot\boldsymbol{x}_1+b_{\widetilde{N}}\right)\\ \cdots & \cdots & \cdots\\ g\left(\boldsymbol{w}_1\cdot\boldsymbol{x}_N+b_1\right) & \cdots & g\left(\boldsymbol{w}_{\widetilde{N}}\cdot\boldsymbol{x}_N+b_{\widetilde{N}}\right)\end{bmatrix}_{N\times\widetilde{N}}
\end{aligned} \tag{12}$$

$$\begin{aligned}
\boldsymbol{\alpha}&=\begin{bmatrix}\boldsymbol{\alpha}_1^{\mathrm{T}}\\ \vdots\\ \boldsymbol{\alpha}_{\widetilde{N}}^{\mathrm{T}}\end{bmatrix}_{\widetilde{N}\times m},\\
\mathbf{y}&=\begin{bmatrix}\boldsymbol{y}_1^{\mathrm{T}}\\ \vdots\\ \boldsymbol{y}_N^{\mathrm{T}}\end{bmatrix}_{N\times m}
\end{aligned} \tag{13}$$

When $g(x)$ is infinitely differentiable, not all the network parameters need to be adjusted, the input weights $\boldsymbol{w}$ and bias $\boldsymbol{b}$ of the hidden layer can be randomly selected during training. Then the determination of the output weights is to find the least square solution with minimum norm to the linear system (11) which can be expressed as

$$\widetilde{\boldsymbol{\alpha}}=\boldsymbol{H}^{+}\boldsymbol{y}=\left(\boldsymbol{H}^{\mathrm{T}}\boldsymbol{H}\right)^{-1}\boldsymbol{H}^{\mathrm{T}}\boldsymbol{y} \tag{14}$$

Finally, the output of ELM is

$$\widetilde{\boldsymbol{y}}=\boldsymbol{H}\widetilde{\boldsymbol{\alpha}}=\widetilde{f}\left(\boldsymbol{x}\right) \tag{15}$$

After identification and validation, apply the identified gas generator state assessment model to engine installed condition.

3.3. Specific Research Process on Initial Installed Power Loss. As the takeoff state of the helicopter is the critical state for monitoring, so the study mainly focuses on the corresponding engine installed power loss at three installed positions. Flight data of the ground takeoff state under the condition that the engine initial installed flight time is 50 hours are selected as the test data. The data extraction and processing method of the takeoff state is as follows: Determine the flight state information based on flight data file, keep the pitch angle and the tilt angle stable, the landing gear wheel-carrier signal is turned off (being 1), and the radio altitude is greater than 0, and make sure the above conditions are satisfied; after that, determine the "pitch position" at the maximum rate of change (first peak) position, 10 seconds delay from this position, and the data that is continuously stable for 5 seconds are selected; remove the maximum and minimum values for each parameter; the remaining data are averaged as the data under the takeoff state. In addition, since the rotor speed NR1 is measured in the actual flight condition and the output shaft torque is presented as a percentage of the limit torque value ($2108.4N\cdot m$), the actual engine output shaft power P_r^{zj} needs to be calculated through the following formulas:

$$n_r=NR1\times 28.57 \tag{16}$$

$$C=M\times 2108.4 \tag{17}$$

$$P_r^{zj}=\frac{n_r\times C}{9550} \tag{18}$$

where n_r is the engine output shaft speed, 28.57 is gear ratio of the main reducer, M represents the percentage of torque limit value, and C is the actual torque value. For ease of comparison, the selected flight data also need to be converted to the standard atmospheric condition.

Input converted gas generator rotor speed $n_{g,c}^{zj}$ in the test data to the model to obtain the corresponding output parameters: converted gas turbine power $P_{gt,c}^{zj}$ and converted gas turbine outlet temperature $T_{5s,c}^{zj}$. For the same engine, data of steady state on engine bench acceptance test condition are selected according to the condition that converted engine output shaft power $P_{r,c}^{zj}$ at the takeoff state under engine installed condition is equal to converted engine output shaft power $P_{r,c}^{tj}$ on engine bench acceptance test condition, and input converted gas generator rotor speed $n_{g,c}^{tj}$ from the selected data to the model to obtain the corresponding output parameters: converted gas turbine power $P_{gt,c}^{tj}$ and converted gas turbine outlet temperature $T_{5s,c}^{tj}$ as well. Through calculation and comparative analysis, the engine initial installed gas turbine power loss P_{ss} is achieved.

$$P_{ss}=\frac{P_{gt,c}^{zj}-P_{gt,c}^{tj}}{P_{gt,c}^{zj}}\times 100\% \tag{19}$$

In summary, the specific research process of initial installed power loss of a certain type of turbo-shaft engine based on QPSO and ELM can be illustrated as in Figure 3.

Step 1 (initializing). First, a population of candidate solutions is generated, and all elements in the particle $\boldsymbol{X_i}=[\pi_{gt,i},\eta_{gt,i}]$ are initialized randomly within the range of $(0, 1)$.

Step 2 (calculation of gas generator performance). The real values of elements in each particle, along with the selected data of steady states in engine bench test, are inputted to the aerodynamic thermal model of gas generator to get the values of T_5, P_{gt} and P_c.

Step 3 (calculation of fitness function value). In combination with the data T_{5s} and P_f of the same steady state, the fitness function value is obtained using (5). If $F(\boldsymbol{X}_i)<\sigma=0.001$

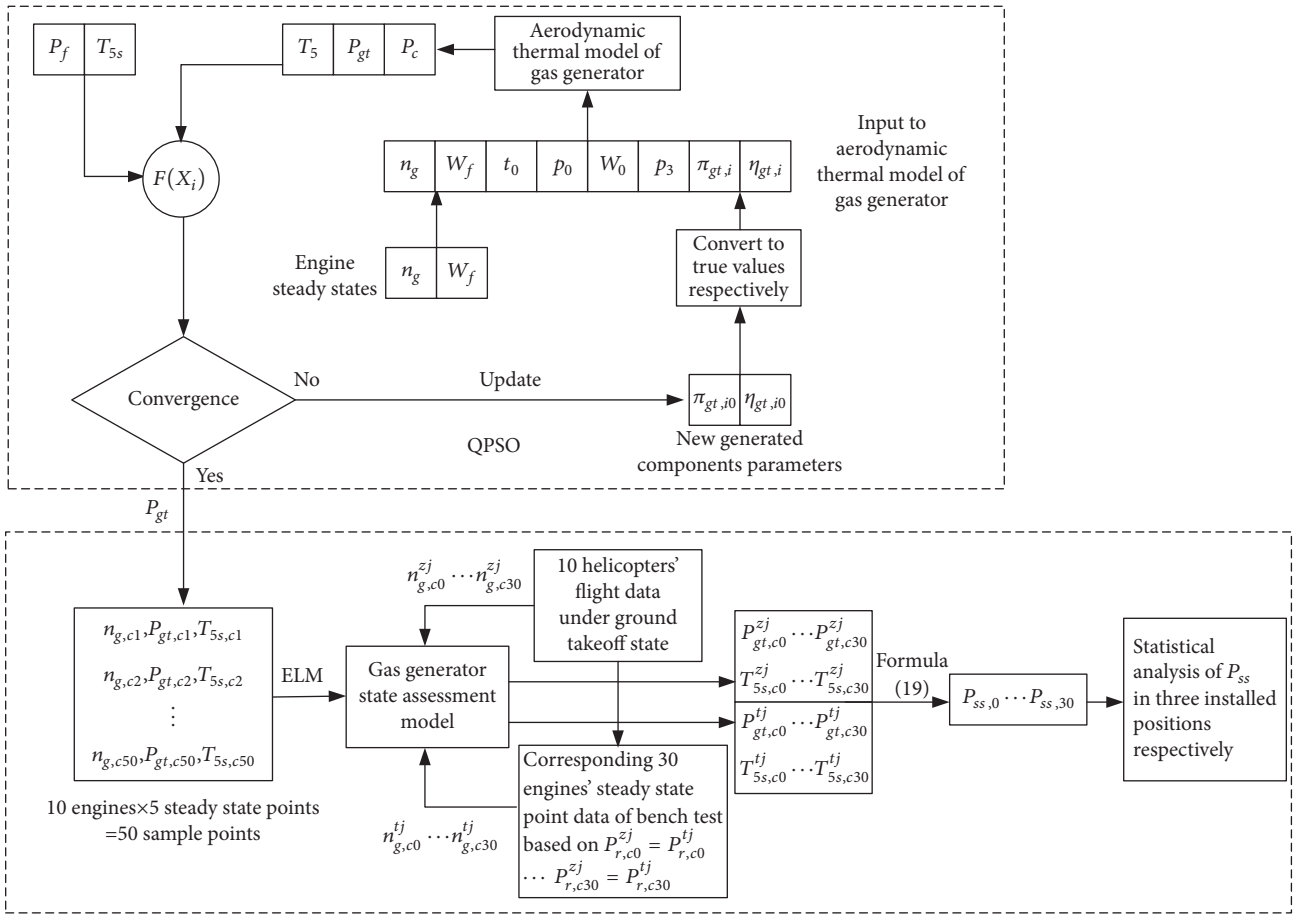

Figure 3: Specific research process of initial installed power loss using QPSO and ELM.

(or the maximum number of iterations is reached), output the optimal solution and calculate P_{gt}; otherwise, QPSO generates a new population of particles and returns to Step 2 to repeat the calculation process. After the optimized calculation, P_{gt} of a steady state can be obtained.

Step 4 (identification of gas generator state assessment model). 10 turbo-shaft engines of the same type are selected, and optimized calculations are carried out for 5 typical steady states of each engine, respectively. After data conversion, a total of 50 sample data points make up the sample sets to identify the gas generator state assessment model using ELM.

Step 5 (apply the identified gas generator state assessment model to engine installed condition). A total of 30 engines of the same type from 10 helicopters are selected as research objects, and flight data of the ground takeoff state under the condition that each engine's initial installed flight time is 50 hours are selected as the test data. After data extraction and processing, input converted gas generator rotor speed $n_{g,c0}^{zj} \cdots n_{g,c30}^{zj}$ in the test data to the model to obtain the corresponding outputs: converted gas turbine power $P_{gt,c0}^{zj} \cdots P_{gt,c30}^{zj}$ and converted gas turbine outlet temperature $T_{5s,c0}^{zj} \cdots T_{5s,c30}^{zj}$. For each engine, data of steady state on engine bench acceptance test condition are selected according to the condition that converted engine output shaft power at the ground takeoff state under engine installed condition is equal to converted engine output shaft power on engine bench acceptance test condition, that is $P_{r,c0}^{zj} = P_{r,c0}^{tj} \cdots P_{r,c30}^{zj} = P_{r,c30}^{tj}$. And input $n_{g,c0}^{tj} \cdots n_{g,c30}^{tj}$ from the selected engine bench acceptance test data to the model to obtain the corresponding outputs: $P_{gt,c0}^{tj} \cdots P_{gt,c30}^{tj}$ and $T_{5s,c0}^{tj} \cdots T_{5s,c30}^{tj}$ as well.

Step 6 (statistical analysis of P_{ss} at three installed positions). In the light of (19), initial installed gas turbine power loss of the selected 30 engines $P_{ss,0} \cdots P_{ss,30}$ is achieved through calculation, and P_{ss} of 10 engines from each installed position are statistically analyzed.

4. Calculation Results and Statistical Analysis

4.1. Calculation Results of Gas Turbine Power at Selected Steady States. According to the above specific research steps, set the basic parameters of QPSO, which mainly include the number of particles in population is 30 and the maximum number of iterations is 30. Then, QPSO can be adopted for the optimized calculation of P_{gt} and T_5 of each steady state from 10 turbo-shaft engines, among them, bench acceptance

Table 2: Data of typical steady states and the corresponding performance calculated results.

Engine	n_g/ (r/min)	W_f/ (L/h)	T_0/ (°C)	p_0/ (Pa)	W_0/ (kg/s)	π_c/ (-)	P_r/ (kW)	T_{5s}/ (°C)	T_5/ (°C)	P_{gt}/ (kW)
1	26819.7	270.38	11.4	102533	5.038	3.825	385.9	491.7	485.6	860.6
	30046.7	402.745	11.8	102539	5.788	5.024	777.5	585.5	591.7	1216
	31032.4	451.931	11.2	102519	6.164	5.466	931.4	618.5	623.4	1400.8
	32519.9	556.208	11.2	102503	6.677	6.12	1231.4	709.7	704	1631.5
	33025.3	592.828	11.1	102519	6.824	6.325	1330	735.9	728.9	1719.1
2	25024.1	211.953	21.8	101660	4.294	3.146	229.4	472.3	466.5	659.6
	30021.8	374.736	21.5	101650	5.556	4.776	686.5	587.7	588.6	1174.4
	31712.4	469.258	21.2	101650	6.143	5.473	956.9	664.3	657.7	1448.4
	32924.1	551.137	21.3	101636	6.532	5.988	1198.8	727.2	722.7	1641.2
	33405.1	584.424	21.2	101629	6.679	6.205	1290.1	752.5	745.5	1704.6
3	25055.8	224.408	9.6	102250	4.505	3.311	253.1	452.3	448.3	691.9
	30030.6	398.017	9.5	102257	5.796	5.033	767.3	598.5	593.5	1214.9
	31731.4	496.431	9.2	102257	6.397	5.756	1071.1	689.9	686.7	1480.2
	32398.5	539.857	9.1	102271	6.623	6.053	1204.5	728.5	722.6	1608.7
	33234.8	586.745	9.0	102277	6.859	6.403	1357.8	771.6	766.1	1732.8

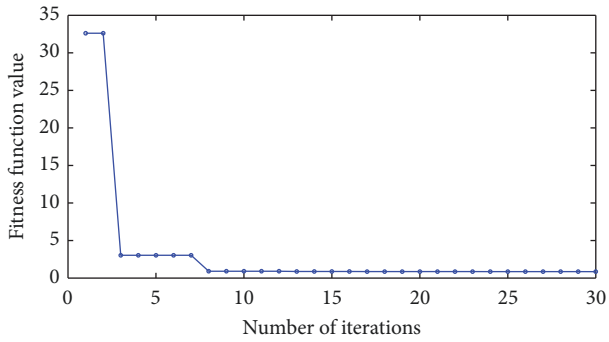

Figure 4: Change of fitness function value.

test data of 5 typical steady states and the corresponding performance calculated results of three engines installed in a helicopter are listed in Table 2, and change of fitness function value of a certain steady state in the optimization process is demonstrated in Figure 4.

It can be seen from Table 2 that the maximum absolute deviation between the actual measured value and the optimized calculation value of gas turbine outlet temperature for each steady state of the three turbo-shaft engines is 7°C, the average absolute deviation is 5.22°C, and the maximum relative deviation is 1.241%. Taking the influence of data acquisition accuracy and other factors into account, the optimized calculation results are very close to the actual values. In combination with the better convergence effect of the fitness function in the optimization process which is demonstrated in Figure 4, the accuracy of gas turbine power obtained by optimized calculation at each steady state is further verified.

4.2. Calculation Results of Initial Installed Gas Turbine Power Loss. Training and validation sample sets of gas generator state assessment model are formed by converting the data of n_g, P_{gt} and T_{5s} from each steady state to standard atmospheric condition, and then ELM is applied to carry out regressive identification of the model. Due to the large difference in the range of values of different parameters, the data of sample sets need to be normalized, and restore the data of each parameter after the training and validation. Apply the identified gas generator state assessment model to engine installed condition. According to the flight data extraction and processing method of ground takeoff state under the condition that the engine initial installed flight time is 50 hours, the extracted flight data of the same helicopter and data processing results are listed in Table 3.

Convert the data processing results to standard atmospheric condition. For the same engine, data of steady state on engine bench acceptance test condition are selected according to $P_r^{zj} = P_r^{tj}$. Then input $n_{g,c}^{zj}$ and $n_{g,c}^{tj}$ to the identified gas generator state assessment model; the corresponding outputs $P_{gt,c}^{zj}$, $T_{5s,c}^{zj}$ and $P_{gt,c}^{tj}$, $T_{5s,c}^{tj}$ can be achieved, respectively. P_{ss} of each engine is calculated as well. The detailed results are listed in Table 4.

From Table 4, it is found that when the engine output shaft emits the same power before and after installation, $P_{gt,c}^{zj}$ is greater than $P_{gt,c}^{tj}$, which means that the engine needs to consume more energy after installation; in other words, energy loss is generated. P_{ss} for three installed positions of a certain helicopter are 1.73%, 10.59%, and 4.85%, respectively.

For the ground takeoff state, the critical factor for P_{ss} is the impact of engines' installed positions on the intake air flow of each engine. Figure 5 displays the layout of the sample helicopter power plant; it is seen that the air inlets of engine

Table 3: Extracted flight data of the ground takeoff state and data processing results.

	Torque 1 / (%)	Torque 2 / (%)	Torque 3 / (%)	Rotor speed / (r/min)	Engine speed 1 / (r/min)	Engine speed 2 / (r/min)	Engine speed 3 / (r/min)	Pitch / (°)	Atmospheric static temperature / (°C)
Extracted flight data	62.808	50.891	60.659	206.6	31036	30747	31429	15.1	23.2
	65.739	52.356	64.469	206.1	31297	30971	31416	15	23.2
	66.227	52.794	65.446	207.5	31395	30977	31534	14.7	23.2
	63.101	51.282	63.101	207.4	31068	30747	31405	14.5	23.2
	60.269	47.57	59.878	207.4	30843	30590	31401	14.9	23.2
Data processing results	63.883	51.510	62.743	206.2	31134	30822	31417	14.9	23.2

Table 4: Performance calculation results on engine installed and bench condition.

Engine	$n_{g,c}^{zj}$/ (r/min)	$P_{gt,c}^{zj}$/ (kW)	$T_{5s,c}^{zj}$/ (°C)	$n_{g,c}^{tj}$/ (r/min)	$P_{gt,c}^{tj}$/ (kW)	$T_{5s,c}^{tj}$/ (°C)	P_{ss}/ (%)
1	30643	1289.5	604.784	30516	1267.2	601.086	1.73
2	30336	1260	594.017	29485	1126.6	561.85	10.59
3	30921	1302.2	645.608	30484	1239.1	623.292	4.85

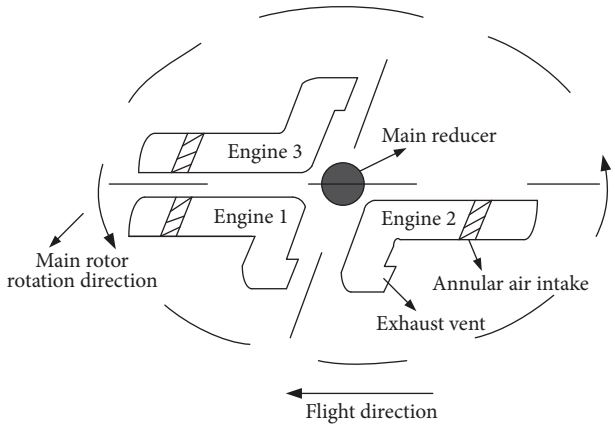

Figure 5: Layout of the sample helicopter power plant.

1 and engine 3 are located on both sides of the fuselage, while the air inlet of engine 2 is located at the upper right of the fuselage and the exhaust system turns to exhaust backwards with the direction of horizontal oblique 30 degrees. From the perspective of relative installed position of the three engines, engine 2 is located behind engine 1 and engine 3, and its exhaust system is in front of the intake system, making the intake airflow vulnerable to the influence of the other two engines, its own exhaust flow field, and the main rotor wake. As a result, the engine performance is affected, so P_{ss} of engine 2 is relatively largest. The doing work capacity of engine 3 is also affected by the dual action of main rotor wake as well as the intake and exhaust flow of engine 2, while engine 1 is less affected by the other two engines, so the performance is relatively stable.

4.3. Statistical Analysis for the Calculation Results in Three Installed Positions. For better quantitative analysis of P_{ss} in three installed positions, a total of 30 engines of the same type from 10 helicopters are selected as the research objects. Initial installed flight data and the corresponding bench test data of each engine are extracted and processed. In combination with the identified gas generator state assessment model, P_{ss} of each engine is obtained through calculation. Then the selected 30 engines are classified in accordance with their installed positions, and statistical analyses are carried out for P_{ss} of 10 engines from each installed position. The serial number of engines in three installed positions are 1-10, 11-20, and 21-30, the performance calculation results of each engine are listed in Tables 5, 6, and 7, respectively. P_{gt} of different engines in bench and installed condition as well as P_{ss} of each engine are intuitively demonstrated in Figures 6 and 7, respectively.

The Shapiro-Wilk W test is a normality test that has been designated as a national standard. It was proposed by Shapiro and Wilk in 1965 and requires a sample size of 3 to 50. This test method can be applied to examine whether a batch of observations or a batch of random numbers come from the same normal distribution [24]. The test question is as follows: H_0, the population obeys normal distribution; H_1, the population disobeys normal distribution.

Statistical analyses are performed on P_{ss} of 10 engines from each installed position. Take P_{ss} of 10 engines in installed position 2; for example, the specific implementation steps are as follows.

(1) Arrange the sample values in nondecreasing order.

$$8.38 \le 8.94 \le 9.01 \le 9.37 \le 9.53 \le 9.87 \le 10.38 \le 10.59 \le 10.75 \le 11.46 \quad (20)$$

Table 5: Performance calculation results of 10 engines in installed position 1.

	The serial number of engines									
	01	02	03	04	05	06	07	08	09	10
$P_{gt,c}^{zj}$(kW)	1289.5	1268.8	1212.6	1237.4	1251.2	1257.2	1315.7	1228.5	1214.3	1276.1
$P_{gt,c}^{tj}$(kW)	1267.2	1245.3	1194.1	1209.4	1228.9	1240.2	1288.9	1205.3	1200.1	1263.6
P_{ss}(%)	1.73	1.85	1.53	2.26	1.78	1.35	2.04	1.89	1.17	0.98

Table 6: Performance calculation results of 10 engines in installed position 2.

	The serial number of engines									
	11	12	13	14	15	16	17	18	19	20
$P_{gt,c}^{zj}$(kW)	1260	1135.8	1202	1217.7	1226.1	1148.6	1258.7	1216.2	1201.6	1198.5
$P_{gt,c}^{tj}$(kW)	1126.6	1029.4	1064.3	1091.3	1115.6	1052.4	1123.4	1096.1	1094.2	1084.3
P_{ss}(%)	10.59	9.37	11.46	10.38	9.01	8.38	10.75	9.87	8.94	9.53

Table 7: Performance calculation results of 10 engines in installed position 3.

	The serial number of engines									
	21	22	23	24	25	26	27	28	29	30
$P_{gt,c}^{zj}$(kW)	1302.2	1342.6	1212.6	1331.5	1243.8	1218.5	1290	1257.3	1223.7	1264.6
$P_{gt,c}^{tj}$(kW)	1239.1	1263.2	1159.9	1239	1195.8	1176.2	1215.8	1205.4	1159.5	1184
P_{ss}(%)	4.85	5.91	4.34	6.95	3.86	3.47	5.76	4.13	5.25	6.37

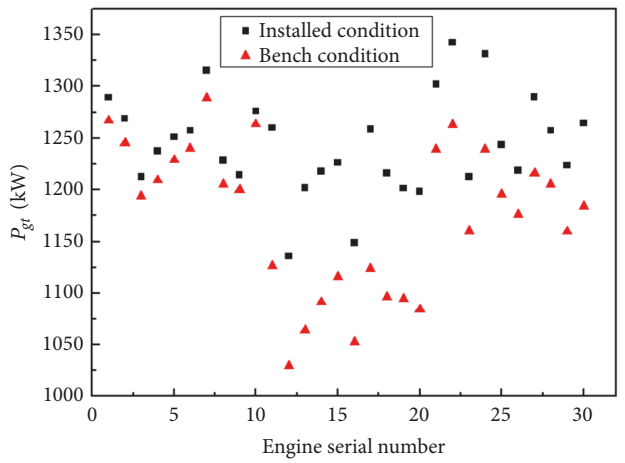

Figure 6: P_{gt} of different engines on bench and installed conditions.

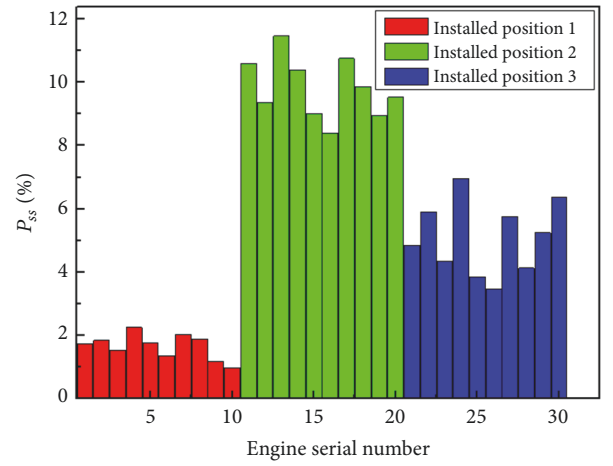

Figure 7: P_{ss} of each engine.

(2) Calculate the value of statistic W using (21). In the formula, $a_k(W)$ is read from schedule 10 in literature [24]. For ease of calculation, the list of values is illustrated as in Table 8.

$$W = \frac{\left\{\sum_{k=1}^{[n/2]} a_k(W)\left[X_{(n+1-k)} - X_{(k)}\right]\right\}^2}{\sum_{k=1}^{n}\left(X_{(k)} - \overline{X}\right)^2} \quad (21)$$

(3) Make a judgment: if $W < W_\alpha$, reject H_0; otherwise accept H_0. Among them, W_α is read from schedule 11 in literature [24] for a given confidence level α and sample size n.

It can be seen from Table 8 that $\sum_{k=1}^{10}(X_{(k)} - \overline{X})^2 = 8.254$, $\sum_{k=1}^{5} a_k(W)[X_{(11-k)} - X_{(k)}] = 2.7426$ and $W = 2.7426^2/8.254 = 0.9113$. For $\alpha = 0.05$, it is found that $W_{0.05} = 0.842$. Owing to $W > W_\alpha$, so accept H_0, and it is considered that P_{ss} at installed position 2 obeys the normal distribution.

Assuming that the population $X \sim N(\mu, \sigma^2)$, μ and σ^2 are mean and variance of the normal population, respectively. P_{ss} of 10 engines in installed position 2 are the samples from the population X. $\overline{X}$ is the sample mean and S^2 is the sample variance. It concludes that $\overline{X}$ is an unbiased estimate of μ, and, on the basis of interval estimation theorem of sample mean from a normal population, a confidence interval with 95% confidence level of μ can be expressed as $(\overline{X} \pm (S/\sqrt{n})t_{\alpha/2}(n-1))$. According to the sample data, it is calculated that

Table 8: The list of values for calculation.

k	$X_{(k)}$	$X_{(11-k)}$	$X_{(11-k)} - X_{(k)}$	$a_k(W)$
1	8.38	11.46	3.08	0.5739
2	8.94	10.75	1.81	0.3291
3	9.01	10.59	1.58	0.2141
4	9.37	10.38	1.01	0.1224
5	9.53	9.87	0.34	0.0399

Table 9: Statistical analysis results of P_{ss} at three installed positions.

Installed position	Performance evaluation index					
	max $\lvert\delta\%\rvert$	medium $\lvert\delta\%\rvert$	min $\lvert\delta\%\rvert$	mean $\lvert\delta\%\rvert$	std ($\delta\%$)	95% confidence interval
1	2.26	1.755	0.98	1.658	0.1428	(1.388%, 1.928%)
2	11.46	9.7	8.38	9.828	0.8254	(9.178%, 10.478%)
3	6.95	5.05	3.47	5.089	1.1924	(4.308%, 5.870%)

$\overline{X} = 9.828$, $S = \sqrt{0.8254} = 0.9085$, $n = 10$ and $t_{0.025}(9) = 2.2622$, then the confidence interval of the mean value of P_{ss} at installed position 2 is obtained as $(9.828 \pm 0.9085/\sqrt{10} \times 2.2622)$, namely (9.178%, 10.478%).

Similarly, the W-normality test and the confidence interval estimation for P_{ss} at installed position 1 and installed position 3 are carried out, respectively.

For installed position 1, $\sum_{k=1}^{10}(X_{(k)} - \overline{X})^2 = 1.428$, $\sum_{k=1}^{5} a_k(W)[X_{(11-k)} - X_{(k)}] = 1.1777$, $W = 1.1777^2/1.428 = 0.9711$, $W > W_{0.05} = 0.842$, so it is considered that P_{ss} at installed position 1 obeys the normal distribution. According to the sample data, it is calculated that $\overline{X} = 1.658, S = \sqrt{0.1428} = 0.3779$, $n = 10$ and $t_{0.025}(9) = 2.2622$, then a confidence interval with 95% confidence level of the mean value of P_{ss} at installed position 1 is obtained as $(1.658 \pm 0.3779/\sqrt{10} \times 2.2622)$, namely, (1.388%, 1.928%).

For installed position 3, $\sum_{k=1}^{10}(X_{(k)} - \overline{X})^2 = 11.924$, $\sum_{k=1}^{5} a_k(W)[X_{(11-k)} - X_{(k)}] = 3.3941$, $W = 3.3941^2/11.924 = 0.9661$, $W > W_{0.05} = 0.842$, so it is considered that P_{ss} at installed position 3 obeys the normal distribution. According to the sample data, it is calculated that $\overline{X} = 5.089, S = \sqrt{1.1924} = 1.092$, $n = 10$ and $t_{0.025}(9) = 2.2622$, then a confidence interval with 95% confidence level of the mean value of P_{ss} at installed position 3 is obtained as $(5.089 \pm 1.092/\sqrt{10} \times 2.2622)$, namely, (4.308%, 5.870%).

In summary, Table 9 lists the statistical analysis results of P_{ss} at three installed positions. The boxplots of P_{ss} at three installed positions is demonstrated in Figure 8.

It is concluded from Table 9 and Figure 8 that the mean value of P_{ss} at three installed positions of a certain type of ship-borne helicopter are 1.658%, 9.828%, and 5.089%, respectively. On the basis of sample estimation, a confidence interval with 95% confidence level of the mean value of P_{ss} at three installed positions are (1.388%, 1.928%), (9.178%, 10.478%), and (4.308%, 5.870%), which are important references for determining the power monitoring thresholds after engine installation.

In addition, statistical calculations have found that gas turbine outlet temperature of the engines rise in all three installed positions due to the increased energy consumption caused by P_{ss}. Although the maximum temperature limit is still not exceeded, the usage time of the engine in large states and the life of components have been affected to a certain extent. With the increase of engine using time, the engine performance will decline, and the value of gas turbine outlet temperature will further increase. It should be monitored with emphasis.

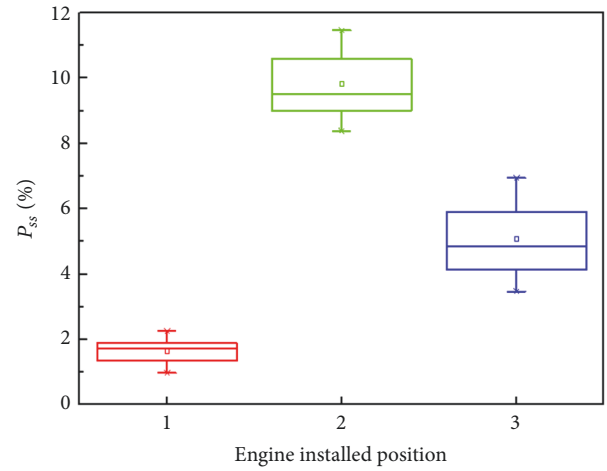

Figure 8: Boxplots of P_{ss} at three installed positions.

5. Conclusions

In this paper, initial installed gas turbine power loss of a certain type of turbo-shaft engine has been studied using data mining and statistical approach, in which QPSO is employed to optimize the calculation of gas turbine power at different steady states based on component-level aerodynamic thermal model of gas generator, then ELM is adopted for regressive identification of the established gas generator state assessment model, and the identification model is applied to engine installed condition, and finally statistical analysis of engine initial installed gas turbine power loss at three

installed positions are performed. The following conclusions can be drawn.

(1) The values of engine initial installed gas turbine power loss at three installed positions all conform to the normal distribution; the mean values are 1.658%, 9.828%, and 5.089% according to the sample estimation, and confidence intervals with 95% confidence level of the mean values are (1.388%, 1.928%), (9.178%, 10.478%), and (4.308%, 5.870%), respectively.

(2) The doing work capacity of engines after initial installation in three installed positions has declined to varying degree, among them, the initial installed gas turbine power loss of engine 2 is relatively largest, for the reason that engine 2 is located behind engine 1 and engine 3 and the exhaust system is in front of the intake system, making the intake airflow vulnerable to the influence of the other two engines, its own exhaust flow field and the main rotor wake so that the engine performance is affected. As for engine 3, it is also affected by the dual action of main rotor wake as well as the intake and exhaust flow of engine 2, while engine 1 is less affected by the other two engines and the performance is relatively stable.

Some of the future research directions are (i) to get more accurate results based on more sample data, (ii) to analyze the effects of different flight states and flight environment on engine installed power loss, and (iii) to discuss the change of engine installed power loss under different engine using time.

Nomenclature

t_0: Atmospheric temperature (°C)
p_0: Atmospheric pressure (Pa)
W_f: Fuel consumption of combustion chamber (L/h)
W_0: Intake air flow (kg/s)
p_3: Total pressure of compressor outlet (Pa)
n_g: Gas generator rotor speed (r/min)
P_{gt}: Gas turbine power (kW)
P_c: Power absorbed by the compressor (kW)
P_f: Power consumed by front-end accessories (kW)
T_5: Calculated value of gas turbine outlet temperature (°C)
T_{5s}: Measured value of gas turbine outlet temperature (°C)
n_r: Engine output shaft speed (r/min)
$n_{g,c}^{zj}$: Converted gas generator rotor speed on engine installed condition (r/min)
$P_{gt,c}^{zj}$: Converted gas turbine power on engine installed condition (kW)
$T_{5s,c}^{zj}$: Converted gas turbine outlet temperature on engine installed condition (°C)
$P_{r,c}^{zj}$: Converted engine output shaft power on engine installed condition (kW)
$P_{r,c}^{tj}$: Converted engine output shaft power on engine bench condition (kW)
$n_{g,c}^{tj}$: Converted gas generator rotor speed on engine bench condition (r/min)
$P_{gt,c}^{tj}$: Converted gas turbine power on engine bench condition (kW)
$T_{5s,c}^{tj}$: Converted gas turbine outlet temperature on engine bench condition (°C)
P_{ss}: Engine initial installed gas turbine power loss (%)
π_{gt}: Gas turbine pressure-drop ratio (-)
η_{gt}: Gas turbine efficiency (-).

Data Availability

The engine bench test data and flight data used to support the findings of this study were supplied by the 370 Factory and PLA 91911 Unit under license and so cannot be made freely available. Requests for access to these data should be made to the confidential sectors of the 370 Factory and PLA 91911 Unit.

Conflicts of Interest

The authors declare that there are no conflicts of interest regarding the publication of this paper.

Acknowledgments

Thanks are due to the special funds of Taishan Scholar Project for the financial support. And also this study was supported by the National Natural Science Foundation of China (Grants nos. 51505492 and 61174031).

References

[1] X. M. Shan, J. Q. Huang, W. X. Zhou et al., "Study and test validation of turbo-shaft engine on-line performance monitoring technology," *Journal of Aerospace Power*, vol. 28, no. 4, pp. 721–729, 2013 (Chinese).

[2] H. Yu, H. Sun, L. Yan, and K. Zhang, "Study on the Condition Monitoring System of Certain Type of Turboshaft Engine Based on Flight Data," in *Proceedings of the First Symposium on Aviation Maintenance and Management-Volume I*, vol. 296 of *Lecture Notes in Electrical Engineering*, pp. 227–234, Springer Berlin Heidelberg, Berlin, Heidelberg, 2014.

[3] L. Shen, Q. Yu, and J. H. Zheng, "Flight test study on the engines power loss of helicopter," *Aeronautical Science and technology*, vol. 26, no. 3, pp. 39–43, 2015.

[4] J. B. Cai and B. A. Hu, "Analysis of technical characteristics of high-power turbo-shaft engine used by heavy helicopter," Tech. Rep., 2014.

[5] P. Gao and W. Dong, "Optimal analysis of flow parameters for marine gas turbine intercooler," *Aeroengine*, vol. 37, no. 4, pp. 29–32, 2011 (Chinese).

[6] K. Coban, C. O. Colpan, and T. H. Karakoc, "Application of thermodynamic laws on a military helicopter engine," *Energy*, vol. 140, pp. 1427–1436, 2017.

[7] Z. C. Zhu, *Research on turbo-shaft engine model correction and control method [PhD. Thesis]*, Nanjing University of Aeronautics and Astronautics, Nanjing, China, 2016.

[8] Ö. Turan and H. Aydın, "Numerical calculation of energy and exergy flows of a turboshaft engine for power generation and helicopter applications," *Energy*, vol. 115, pp. 914–923, 2016.

[9] H. L. Sheng, T. H. Zhang, and W. Jiang, "Full-range mathematical modeling of turbo-shaft engine in aerospace," *International Journal of Turbo & Jet Engines*, vol. 33, no. 4, pp. 1–9, 2015.

[10] Q. Zhao, Y. C. Chen, Y. W. Wang et al., "Study of mathematical model on steady-characteristics of turbo-shaft engine based on component modeling," *Advances in Aeronautical Science and Engineering*, vol. 2, no. 3, pp. 312–317, 2011.

[11] M Chen, K Zhang, and H.-L. Tang, "A Probabilistic Design Methodology for a Turboshaft Engine Overall Performance Analysis," *Advances in Mechanical Engineering*, vol. 2014, Article ID 976853, 12 pages, 2014.

[12] H.-L. Tang, K. Zhang, K. Guo, and M. Chen, "Quantification method of effects of uncertainty on component performance for turbo-shaft engine performance," *Tuijin Jishu/Journal of Propulsion Technology*, vol. 36, no. 8, pp. 1143–1150, 2015.

[13] D. L. Simon and J. S. Litt, "Automated power assessment for helicopter turbo-shaft engines," *NASA/TM*, Article ID 215270, 2008.

[14] B. Nkoi, P. Pilidis, and T. Nikolaidis, "Performance assessment of simple and modified cycle turboshaft gas turbines," *Propulsion and Power Research*, vol. 2, no. 2, pp. 96–106, 2013.

[15] S. M. Ghoreyshi and M. T. Schobeiri, "Numerical simulation of the multistage Ultra-High Efficiency Gas Turbine Engine, UHEGT," in *Proceedings of the ASME Turbo Expo 2017: Turbomachinery Technical Conference and Exposition, GT 2017*, USA, June 2017.

[16] F. Lu, Y. Ye, and J. Huang, "Gas turbine engine identification based on a bank of self-tuning wiener models using fast kernel extreme learning machine," *Energies*, vol. 10, no. 9, 2017.

[17] P. F. Pan, M. M. Ma, and Y. Z. Xu, "Flight test data-driven model identification of turbofan engine," *Gas Turbine Experiment and Research*, vol. 29, no. 6, pp. 21–25, 2016.

[18] E. Mohammadi and M. Montazeri-Gh, "A New Approach to the Gray-Box Identification of Wiener Models with the Application of Gas Turbine Engine Modeling," *Journal of Engineering for Gas Turbines and Power*, vol. 137, no. 7, 2015.

[19] M. T. Yildirim and B. Kurt, "Aircraft Gas Turbine Engine Health Monitoring System by Real Flight Data," *International Journal of Aerospace Engineering*, vol. 2018, Article ID 9570873, 12 pages, 2018.

[20] Y. Ying, Y. Cao, S. Li, and J. Li, "Nonlinear Steady-State Model Based Gas Turbine Health Status Estimation Approach with Improved Particle Swarm Optimization Algorithm," *Mathematical Problems in Engineering*, vol. 2015, Article ID 940757, 12 pages, 2015.

[21] X. Yang, W. Shen, S. Pang, B. Li, K. Jiang, and Y. Wang, "A Novel Gas Turbine Engine Health Status Estimation Method Using Quantum-Behaved Particle Swarm Optimization," *Mathematical Problems in Engineering*, vol. 2014, Article ID 302514, 11 pages, 2014.

[22] C. W. Deng, G. B. Huang, X. U. Jia et al., "Extreme learning machines: new trends and applications," *Science China Information Sciences*, vol. 58, no. 2, pp. 1–16, 2015.

[23] G.-B. Huang, "What are extreme learning machines? Filling the Gap Between Frank Rosenblatt's Dream and John von Neumann's Puzzle," *Cognitive Computation*, vol. 7, no. 3, pp. 263–278, 2015.

[24] Y. Wu, Y. L Li, and Q. J. Hu, *Applied Mathematical Statistics*, National University of Defense Technology press, Changsha, China, 1995.